# Screening Charged Impurities and Lifting the Orbital Degeneracy in Graphene by Populating Landau Levels

Adina Luican-Mayer,[1] Maxim Kharitonov,[1] Guohong Li,[1] Chih-Pin Lu,[1] Ivan Skachko,[1] Alem-Mar B. Gonçalves,[1] K. Watanabe,[2] T. Taniguchi,[2] and Eva Y. Andrei[1,*]

[1]*Department of Physics and Astronomy, Rutgers University, Piscataway, New Jersey 08854, USA*

[2]*Advanced Materials Laboratory, National Institute for Materials Science, 1-1 Namiki, Tsukuba 305-0044, Japan*

(Received 19 July 2013; published 23 January 2014)

We report the observation of an isolated charged impurity in graphene and present direct evidence of the close connection between the screening properties of a 2D electron system and the influence of the impurity on its electronic environment. Using scanning tunneling microscopy and Landau level spectroscopy, we demonstrate that in the presence of a magnetic field the strength of the impurity can be tuned by controlling the occupation of Landau-level states with a gate voltage. At low occupation the impurity is screened, becoming essentially invisible. Screening diminishes as states are filled until, for fully occupied Landau levels, the unscreened impurity significantly perturbs the spectrum in its vicinity. In this regime we report the first observation of Landau-level splitting into discrete states due to lifting the orbital degeneracy.

DOI: 10.1103/PhysRevLett.112.036804 PACS numbers: 73.22.Pr, 68.37.Ef, 71.70.Di, 73.43.-f

Charged impurities are the primary source of disorder and scattering in two-dimensional electron systems [1]. They produce a spatially localized signature in the density of states (DOS) which, for impurities at the surface, is readily observed with scanning tunneling microscopy and spectroscopy (STM + STS) [2]. In this respect, graphene [3–6] provides a unique playground for elucidating the role of impurities in 2D systems [6–8]. They are particularly important in the presence of a magnetic field when the quantization into highly degenerate Landau levels (LL) gives rise to the quantum Hall effect (QHE). In this regime, charged impurities are expected to lift the orbital degeneracy, causing each LL in their vicinity to split into discrete sublevels [9]. Thus far, however, the sublevels were not experimentally accessible due to the difficulty to attain sufficiently clean samples that would allow isolating a single impurity. Instead, previous experiments [10,11] presented a picture of bent levels which could be interpreted semiclassically in terms of electronic drift trajectories moving along the equipotential lines defined by a dense distribution of charged impurities.

In this work we employed high quality gated graphene devices to access the electronic spectrum in the QHE regime in the presence of an isolated charged impurity. We demonstrate that the strength of the impurity can be controlled by tuning the LL occupation with a backgate voltage. For almost empty LLs the impurity is screened and essentially invisible, whereas at full LL occupancy screening is very weak and the impurity attains maximum strength. In the unscreened regime we resolve the discrete quantum-mechanical spectrum arising from lifting the orbital degeneracy.

The low energy spectrum of pristine graphene gives rise to a linear DOS, which vanishes at the charge neutrality point (CNP). In the presence of a magnetic field $B$, the spectrum is quantized into a sequence of LLs characteristic of massless Dirac fermions:

$$E_N = \pm \frac{\hbar v_F}{l_B} \sqrt{2|N|}, \qquad N = 0, \pm 1, \pm 2, \ldots, \quad (1)$$

where $v_F$ is the Fermi velocity, $l_B = \sqrt{\hbar/eB}$ is the magnetic length, $-e$ is the electron charge, $\hbar = h/2\pi$, $h$ is the Planck constant, and $\pm$ refers to electron (hole) states with LL index $N > 0$ ($N < 0$). We employed LL spectroscopy [5] to study the electronic properties of graphene and their modification in the presence of a charged impurity. The LL spectra were obtained by measuring the bias voltage dependence of the differential tunneling conductance, $dI/dV$, which is proportional to the local DOS, $D(E, \mathbf{r})$ at the tip position $\mathbf{r}$. Here, $V = (E - E_F)/e$ is the bias voltage and $E$ the energy measured relative to the Fermi level $E_F$.

Samples were prepared by exfoliating graphene from analyzer-grade HOPG and deposited on a doped Si backgate capped with 300 nm of chlorinated $SiO_2$ [12]. To achieve high quality we used two superposed graphene layers twisted away from Bernal stacking by a large angle. This ensures that the spectrum of single layer graphene (SLG) is preserved [13,14] while reducing the random potential fluctuations due to substrate imperfections. Hexagonal boron nitride ($h$-BN) flakes, which significantly reduce the corrugation of graphene [15], were also employed [Fig. 1(a)], but the data reported are restricted to the $SiO_2$ substrate.

Using the STM tip as a capacitive antenna [16], we located the samples at low temperature and performed STS to identify areas of interest. A typical zero-field spectrum taken far from an impurity in Fig. 1(b) reveals the V-shaped DOS characteristic of SLG. In finite field the spectrum develops pronounced peaks [Fig. 1(c)] at energies

 

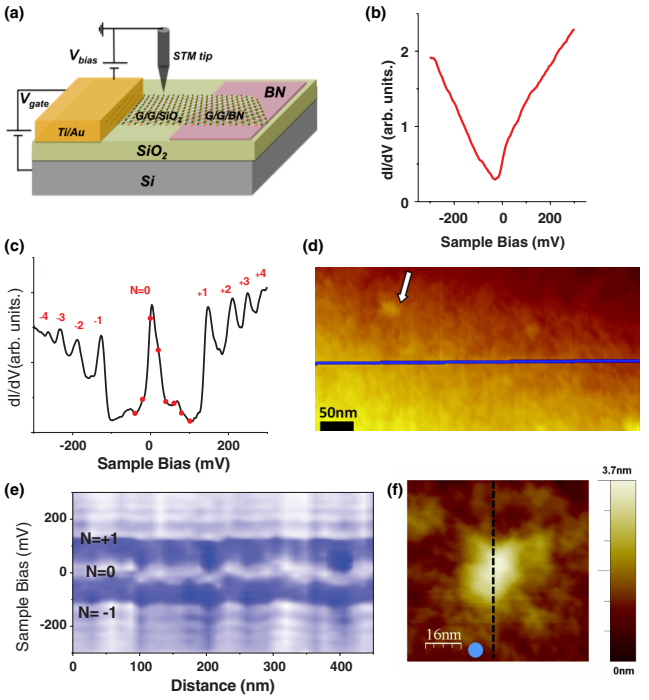


FIG. 1 (color online). (a) Schematics of gated graphene device illustrating the two stacked graphene layers deposited on $SiO_2$ and on $h$-BN in $(G/G/SiO_2)$ and $(G/G/BN)$. The graphene layers share the same electrode. (b) Zero-field STS far from the impurity. (c) STS at $B = 10$ T and $V_g = 0$ V shows well-resolved quantized LLs. (d) Topographic image indicating the line where the spectra in (e) were taken and the position of the isolated impurity. (e) STS line cut along the line shown in (d); $N = 0$ is clearly resolved. (f) STM topography zoom into area with isolated impurity ($V_B = 250$ mV, $I_t = 20$ pA).

corresponding to the LLs [17] that are well resolved up to $N = 4$ in both electron and hole sectors, attesting to good sample quality. Fitting the field and level index dependence to Eq. (1) confirms the massless Dirac-fermion nature of the quasiparticles with $v_F = 1.2 \times 10^6\ m/s$, consistent with measurements on SLG. Charged impurities were located using LL spectroscopy to measure the separation between $E_F$ and the CNP, which coincides with the $N = 0$ level. LL spectroscopy is more sensitive to the position of the CNP than the broad zero-field spectrum. The search for impurities starts with a topography image [Fig. 1(d)] followed by STS. An intensity map of the LLs as a function of position [Fig. 1(e)] shows the fluctuations of the $N = 0$ level in response to charged impurities. Zooming into this area the impurity appears as an isolated bright region in the center of Fig. 1(f). To visualize its effect on the spatial distribution of the electronic wave function, we measured constant energy DOS maps (Fig. 2). The maps are roughly radially symmetric, consistent with a charged impurity at the center. We note that for energies within a gap between LLs, the electronic DOS (bright region) is tightly localized on the impurity. In contrast, for energies in the center of the LL the electronic DOS extends across the entire field of view while avoiding the impurity. This fully supports the picture which attributes the QHE plateaus to the existence of localized impurity states in the gaps between LLs.

We next studied the effect of LL occupancy (filling) by tuning the gate voltage $V_g$ to progressively fill the LLs. The LL filling factor is $\nu = n/n_0(B)$, where $n \approx 7 \times 10^{10} V_g\,[\mathrm{Volts}]\ \mathrm{cm}^{-2}$ is the carrier density and $n_0(B) = g_l g_v g_s (Be/h)$ is the degeneracy per area of the LL. Here $g_l = g_v = g_s = 2$ represent the layer, valley, and spin degeneracy, respectively. Placing the STM tip far from the impurity, we find that as $V_g$ is swept, the LL peaks produce a distinctive steplike pattern seen as bright traces in the intensity map of Fig. 3(a) [12,18]. Each step consists of a nearly horizontal plateau separated from its neighbors by steep slopes. The separation between the centers of steep segments, $\Delta V_g \approx 28$ V, gives the LL degeneracy $\approx 2 \times 10^{12}\ \mathrm{cm}^{-2}$ for $B = 10$ T, as expected for this double-layer sample [19]. The plateau indicates that the Fermi energy remains pinned within a narrow energy band around the center of the LL until the plateau states are filled. A further increase in $V_g$ populates the sparse states in the gap producing the steep slopes [20].

To explore the influence of the impurity on the LLs, we follow the spatial evolution of spectra along a trajectory traversing it [Fig. 1(f)] for a series of gate voltages. As shown in Fig. 3(b), for certain gate voltages the spectra become significantly distorted close to the impurity, with the $N = 0$ level shifting downwards toward negative energies. The downshift indicates an attractive potential produced by a positively charged impurity. Its strength, as measured by the distortion of the $N = 0$ LL, reveals a surprisingly strong dependence on LL filling. In the range of gate voltages corresponding to filling the $N = 0$ LL ($-15 < V_g < 9$ V), the distortion grows monotonically with filling. At small filling it is almost absent, indicating that the impurity is effectively screened and it reaches its maximum value close to full occupancy. At full occupancy the $N = 0$ level shifts by as much as $\approx 0.1\ eV$, indicating that the effect would survive at room temperature. We note that this distortion is only present in the immediate vicinity of the impurity. Farther away no distortion is observed for all the carrier densities studied here.

We attribute the variation of the impurity strength with filling to the screening properties of the electron system. For a positively (negatively) charged impurity and almost empty (full) LLs, unoccupied states necessary for virtual electron transitions are readily available in the vicinity of the impurity, resulting in substantial screening. In contrast, for almost filled (empty) LLs, unoccupied states are scarce, which renders local screening inefficient [21]

Remarkably, when screening is minimal ($V_g = 7$ V) the $N = 0$ LL does not shift smoothly, but rather splits into a series of well-resolved discrete spectral lines in the immediate vicinity of the impurity. As shown in Figs. 4(a) and 4(b), the evolution of the spectra radially outwards from the

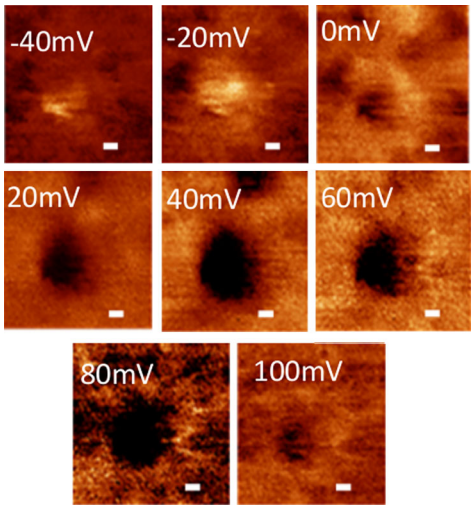


FIG. 2 (color online). Spatial $dI/dV$ maps at $B = 10$ T near the impurity taken at indicated bias voltages. Scale bar for all maps is 8.2 $nm = l_B$.

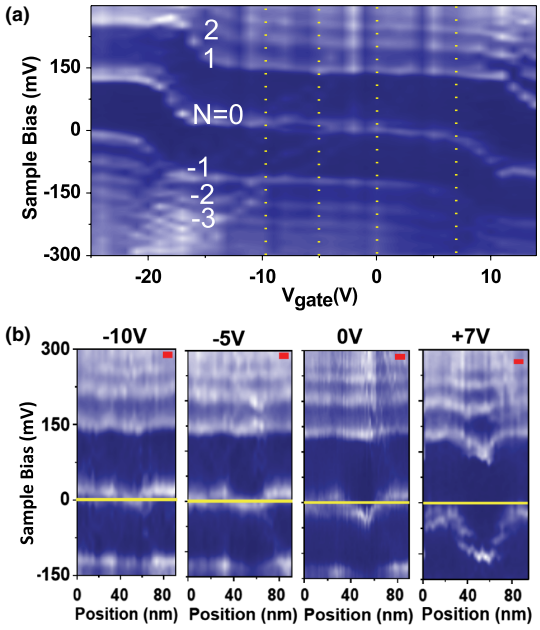


FIG. 3 (color online). Impurity screening by populating Landau levels. (a) DOS map at $B = 10$ T showing evolution of LLs as a function of gate voltage taken far from the impurity at the position indicated by the blue dot in Fig. 1(f). Dashed lines indicate gate voltages of the spectra in (b). (b) DOS line cuts across the impurity for indicated gate voltages. The distortion of the LL sequence by the impurity is strongest for filled levels ($V_g = +7$ V), diminishing as filling is reduced and becoming negligible at $V_g = -10$ V.

center of the impurity exhibits a progression of peaks within the $N = 0$ LL. Starting with a single peak at the center of the impurity, it evolves into a well-resolved double peak and then a triplet at distances ≈13 and 20 nm from the center, respectively. This behavior can be understood by considering the quantum-mechanical electron motion in the presence of a magnetic field and a charged impurity. In one valley and for each spin projection, the two-component wave function $\psi = (\psi_A, \psi_B)^T$ satisfies an effective Dirac Hamiltonian: $\hat{H}\psi = [v_F \boldsymbol{\sigma} \cdot (\boldsymbol{p} - e\boldsymbol{A}) + U(r)]\psi = E\psi$, where, $\boldsymbol{\sigma} = (\sigma_x, \sigma_y)$ are the Pauli matrices in the sublattice space, $\boldsymbol{p} = -i\hbar\nabla$, $\mathbf{B} = \nabla \times \boldsymbol{A}$, and $\mathbf{A} = (1/2)[\mathbf{B} \times \mathbf{r}]$ is the vector potential. We assume a radially symmetric impurity potential $U(r)$ and neglect spin. In the symmetric gauge the eigenstates are characterized by the orbital quantum number $m$. For the unperturbed spectrum in Eq. (1), the eigenfunctions are $\psi^0_{NmA}(r)$, $\psi^0_{NmB}(r)$ [Fig. 4(c)], where $m \geq -|N|$. Since $E_N$ are independent of $m$, the LLs have infinite orbital degeneracy. The impurity lifts this orbital degeneracy and the eigenenergies split into series of sublevels $E_{Nm}$.

To illustrate impurity-induced orbital splitting, we numerically solved the problem for a Coulomb potential $U(r) = (Z/\kappa)(e^2/4\pi\epsilon_0)(1/\sqrt{r^2 + a^2})$ corresponding to a charge $Z$ located a distance $a$ below the graphene plane with $\kappa$ the effective dielectric constant and $\epsilon_0$ the permittivity of free space. The resulting simulated spectrum in Fig. 4(d) shows that the orbital degeneracy is lifted, resulting in an $m$ dependent energy downshift. The downshift is largest for $E_{00}$, and diminishes with increasing $m$ and/or $N$, where the unperturbed LLs are approached. For comparison with the STS data, we calculated the local tunneling DOS assuming a finite linewidth $\gamma$ [22]. If $\gamma < \Delta E_{Nm}$ ($\Delta E_{Nm}$ spacing between adjacent levels), the discreteness of the spectrum is resolved, but for $\gamma \geq \Delta E_{Nm}$, peaks of adjacent states overlap and merge into a continuous band.

Thus, even if the spectrum is discrete, but the resolution is insufficient or if impurities are too close together, the measured $D(E, \mathbf{r})$ will still display "bent" LLs, whose energies seemingly adjust to the local potential. The resulting $D(E, \mathbf{r})$, shown in Fig. 4(d), captures the main features of the data. Upon approaching the impurity, the $N = 0$ LL splits into discrete peaks, attributed to specific orbital states. In both experiment and simulation the states $\psi_{0m}(\mathbf{r})$ with $m = 0, 1, 2$ are well resolved close to the impurity, but higher order states merge into a continuous line. Similarly, the discreteness of the spectrum is not resolved for $N \neq 0$, consistent with the weaker impurity effect at larger distances. We note that for partial filling ($V_g = -5$ and 0 V), as screening becomes more efficient and orbital splitting is no longer observed, the unresolved sublevels merge into continuous lines of bent Landau levels [Fig. 3(b)]. Thus, the capability to tune the strength of the impurity allows us to trace the evolution between the discrete and the previously observed quasicontinuous regimes [11].

We now turn to the effective charge of the impurity and how its screening is affected by LL occupancy. Although we do not have *in situ* chemical characterization of the impurity, we can assume, based on chemical analysis of similar samples, that the most likely candidate consistent with our

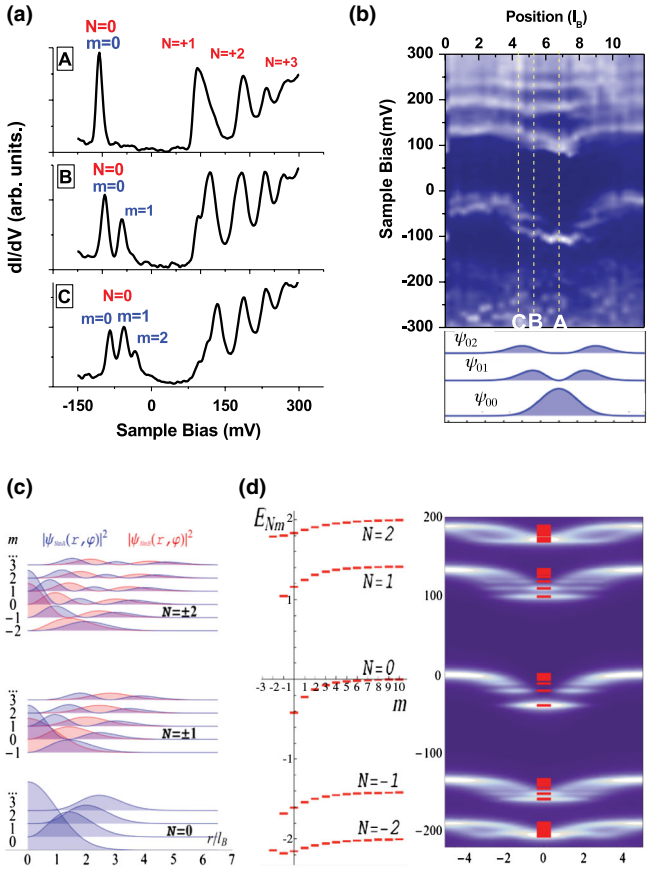


FIG. 4 (color online). Lifting the orbital degeneracy of LLs. (a) $dI/dV$ spectra for $B = 10$ T and $V_g = 7$ V at the positions indicated in (b) reveal peaks corresponding to $N = 0$ and $m = 0$, $m = 0$, 1, and $m = 0, 1, 2$. (b) Top: LL map across the impurity for $V_g = 7$ V. Dashed lines at 0, 13, and 20 nm from the center of the impurity indicate the position of the spectra in (a). Bottom: Calculated probability densities for $\psi_{0m}$ with $m = 0, 1, 2$ are consistent with the spatial distribution of the spectral lines in the top panel. (c) Calculated probability densities on the two graphene sublattices $A$ (blue) and $B$ (red). (d) Left: Simulated spectrum near an impurity illustrating lifting the orbital degeneracy in different LLs. Right: Simulated DOS near an impurity. Linewidth $\gamma = 0.05 v_F/l_B$. Red lines represent calculated energies $E_{Nm}$ shown in the left-hand panel.

observations is a $Na^+$ ion adsorbed on the surface of the $SiO_2$ substrate [23]. It is well known that $Na^+$ ions are ubiquitous in clean rooms and laboratory environments and they are readily adsorbed on $SiO_2$ [24]. For a $Na^+$ ion adsorbed on the substrate underneath the first graphene layer, $a \approx 0.6\ nm \ll l_B$. A rough estimate of its effect on the spectrum can be obtained by equating the measured energy shift $\Delta E_{00} \approx 0.1$ eV, obtained at $V_g = +7$ V, to the calculated value in first-order perturbation theory [25] $\Delta E_{00} \approx (Z/\kappa)(e^2/4\pi\epsilon_0 l_B)(\pi/2)^{1/2}$ which results in $Z/\kappa = 2.5$. Factoring out the contribution of the $SiO_2$ substrate, $\kappa_{SiO_2} = 4$, from the expression for the dielectric constant [26], $\kappa = \kappa_{gr}(\kappa_{SiO_2} + 1)/2$, gives $Z/\kappa_{gr} \cong 1$, where $\kappa_{gr}$ is the static dielectric constant of graphene. This indicates that graphene provides no screening for fully occupied LLs and that the bare charge of the impurity is $Z \cong +1$. In the limit of almost empty LLs ($V_g = -10$ V), the estimated $\kappa_{gr} \approx 5$ indicates that graphene strongly screens the impurity potential [27]. The absence of screening for filled states implies strong Coulomb interactions when $E_F$ lies in a gap consistent with the observation of a fractional QHE in suspended graphene [28].

This work demonstrates that screening in graphene is controlled by LL occupancy and that it is possible to tune charge impurities and their effect on the environment by applying a gate voltage or by varying the magnetic field. Because of the large enhancement of the effective fine-structure constant in graphene, a charged impurity with $Z \geq 1$ is expected to become supercritical [3,8], but tuning the effective charge to observe supercritically is extremely difficult [29]. The ability demonstrated here to tune the strength of the impurity *in situ* opens the door to explore Coulomb criticality and to investigate a hitherto inaccessible regime of criticality in the presence of a magnetic field [9].

Funding provided by DOE-FG02-99ER45742 (E. Y. A. and G. L.), Lucent (A. L.-M.), NSF DMR 1207108 (I. S. and C. P. L.), IAMDN, DOE DE-FG02-99ER45790 (M. K.), and Brazilian agency Capes BEX 5115-09-4 (A.-M. B. G). We thank M. Devoret for useful discussions and M. Aronson for the HOPG crystal.

*Corresponding author.eandrei@physics.rutgers.edu

[1] T. Ando, A. B. Fowler, and F. Stern, Rev. Mod. Phys. **54**, 437 (1982).
[2] H. Mizes and J. Foster, Science **244**, 559 (1989).
[3] A. H. Castro Neto, F. Guinea, N. M. R. Peres, K. S. Novoselov, and A. K.Geim., Rev. Mod. Phys. **81**, 109 (2009).
[4] D. Abergel, V. Apalkov, J. Berashevich, K. Ziegler, and T. Chakraborty, Adv. Phys. **59**, 261 (2010); M. Morgenstern, Phys. Status Solidi B **248**, 2423 (2011).
[5] E. Y. Andrei, G. Li, and X. Du, Rep. Prog. Phys. **75**, 056501 (2012).
[6] V. N. Kotov, B. Uchoa, V. M. Pereira, F. Guinea, and A. H. Castro Neto, Rev. Mod. Phys. **84**, 1067 (2012).
[7] D. V. Khveshchenko, Phys. Rev. B **74**, 161402 (2006); J. Chen, C. Jang, S. Adam, M. Fuhrer, E. Williams, and M. Ishigami, Nat. Phys. **4**, 377 (2008); Y. Zhang, V. Brar, C. Girit, A. Zettl, and M. Crommie, *ibid.* **5**, 722 (2009); T. O. Wehling, S. Yuan, A. I. Lichtenstein, A. K. Geim, and M. I. Katsnelson, Phys. Rev. Lett. **105**, 056802 (2010); C. Bena, Phys. Rev. B **81**, 045409 (2010); S. Das Sarma, S. Adam, E. H. Hwang, and E. Rossi, Rev. Mod. Phys. **83**, 407 (2011).
[8] V. M. Pereira, J. Nilsson, and A. H. Castro Neto, Phys. Rev. Lett. **99**, 166802 (2007); A. V. Shytov, M. I. Katsnelson, and L. S. Levitov, *ibid.* **99**, 246802 (2007).
[9] O. V. Gamayun, E. V. Gorbar, and V. P.Gusynin, Phys. Rev. B **83**, 235104 (2011); Y. Zhang, Y. Barlas, and K. Yang, *ibid.* **85**, 165423 (2012).

[10] A. Yacoby, H. Hess, T. Fulton, L. Pfeiffer, and K. West, Solid State Commun. **111**, 1 (1999); K. Hashimoto, C. Sohrmann, J. Wiebe, T. Inaoka, F. Meier, Y. Hirayama, R. A. Römer, R. Wiesendanger, and M. Morgenstern, Phys. Rev. Lett. **101**, 256802 (2008).

[11] D. Yoshioka, J. Phys. Soc. Jpn. **76**, 024718 (2007); Y. Niimi, H. Kambara, and H. Fukuyama, Phys. Rev. Lett. **102**, 026803 (2009); D. Miller, K. Kubista, G. Rutter, M. Ruan, W. de Heer, M. Kindermann, P. First, and J. Stroscio, Nat. Phys. **6**, 811 (2010); M. Morgenstern, A. Georgi, C. Straßer, C. Ast, S. Becker, and M. Liebmann, Physica (Amsterdam) **44E**, 1795 (2012).

[12] A. Luican, G. Li, and E. Y. Andrei, Phys. Rev. B **83**, 041405 (2011).

[13] J. C. Meyer, A. Geim, M. Katsnelson, K. Novoselov, T. Booth, and S. Roth, Nature (London) **446**, 60 (2007); G. Li, A. Luican, J. L. Dos Santos, A. C. Neto, A. Reina, J. Kong, and E. Andrei, Nat. Phys. **6**, 109 (2009); A. Luican, G. Li, A. Reina, J. Kong, R. R. Nair, K. S. Novoselov, A. K. Geim, and E. Y. Andrei, Phys. Rev. Lett. **106**, 126802 (2011).

[14] A twist between superposed graphene layers gives rise to two peaks in the density of states (van Hove singularities) which flank the charge neutrality point and are separated from each other by an energy which increases with twist angle [13]. For twist angles exceeding 10°, the low energy spectrum (< 1 eV) is indistinguishable from that of single layer graphene. The absence of van Hove singularities and the single layer LL spectrum in the data reported here provide direct evidence of layer decoupling. Although there is no topographic signature of the associated Moiré pattern, which would require a very sharp tip, the above signatures are taken as evidence for a large twist angle.

[15] J. Xue, J. Sanchez-Yamagishi, D. Bulmash, P. Jacquod, A. Deshpande, K. Watanabe, T. Taniguchi, P. Jarillo-Herrero, and B. J. LeRoy, Nat. Mater. **10**, 282 (2011).

[16] G. Li, A. Luican, and E. Y. Andrei, Rev. Sci. Instrum. **82**, 073701 (2011).

[17] G. Li and E. Andrei, Nat. Phys. **3**, 623 (2007); G. Li, A. Luican, and E. Y. Andrei, Phys. Rev. Lett. **102**, 176804 (2009).

[18] O. Dial, R. Ashoori, L. Pfeiffer, and K. West, Nature (London) **448**, 176 (2007).

[19] D. S. Lee, C. Riedl, T. Beringer, A. H. Castro Neto, K. von Klitzing, U. Starke, and J. H. Smet, Phys. Rev. Lett. **107**, 216602 (2011); J. D. Sanchez-Yamagishi, T. Taychatanapat, K. Watanabe, T. Taniguchi, A. Yacoby, and P. Jarillo-Herrero, *ibid.* **108**, 076601 (2012).

[20] Although STM explores only a small area of the sample, the gate-voltage dependence of the data in Fig. 3(a) reflects the available states in the entire sample including those that are outside the field of view of the STM. This is because the gate covers the entire sample and can populate all available states.

[21] These properties are readily understood by examining the local DOS, $D_s(E,r) = \int d^2 r D(E,r)/S$, averaged over a finite-size region $S$ around the impurity. Unlike the DOS averaged over the whole sample, $D_s(E,r)$, is manifestly particle-hole asymmetric within a given LL, which translates to the particle-hole asymmetry of the local screening.

[22] $D(E,r) = 4\sum_{Nm} \delta_\gamma(E - E_{Nm}) \psi^\dagger_{Nm}(r) \psi_{Nm}(r)$. Here, $\delta_\gamma(E - E_{Nm}) = \gamma/\{\pi[(E - E_{Nm})^2 + \gamma^2]\}$ represents the broadened LL. The peak intensity is determined by the probability density $\psi^\dagger_{Nm}(\mathbf{r})\psi_{Nm}(\mathbf{r})$ and is position dependent.

[23] I. Constant, F. Tardif, and J. Derrien, Semicond. Sci. Technol. **15**, 61 (2000).

[24] J. Fripiat, J. Chaussidon, and A. Jelli, *Chimie-physique des phénomènes de surface: Applications aux oxydes et aux silicates* (Masson et Cie éditeurs, Paris, 1971).

[25] $\Delta E_{00} = (Z/\kappa)(e^2/4\pi\epsilon_0 l_B)(\pi/2)^{(1/2)}[1 - Erf(a/l_B)]$, where $Erf(x)$ is the error function.

[26] E. H. Hwang and S. Das Sarma, Phys. Rev. B **75**, 205418 (2007).

[27] This value is comparable to the zero-field RPA estimate by the authors of Ref. [26] for double layer graphene, $\kappa_{gr} = 1 + g_l g_s g_v \pi r_s/8 \approx 3.75$, suggesting that when the LLs are almost empty, screening of positive charges in graphene is comparable to the zero-field case. Here, $r_s = 4\pi e^2/hv_F(\kappa_{SiO_2} + 1)$ is the dimensionless Wigner-Seitz radius which measures the relative strength of the potential and kinetic energies in an interacting quantum Coulomb system with linear dispersion. We note that for single layer graphene, $g_l = 1$, screening would be significantly weaker, $\kappa_{gr} \approx 2.4$.

[28] X. Du, I. Skachko, F. Duerr, A. Luican, and E. Y.Andrei, Nature (London) **462**, 192 (2009); K. I. Bolotin, F. Ghahari, M. D. Shulman, H. L. Stormer, and P. Kim, Nature (London) **462**, 196 (2009).

[29] Y. Wang, V. W. Brar, A. V. Shytov, Q. Wu, W. Regan, H.-Z. Tsai, A. Zettl, L. S. Levitov, and M. F. Crommie, Nat. Phys. **8**, 653 (2012); Y. Wang, D. Wong, A. V. Shytov, V. W. Brar, S. Choi, Q. Wu, H.-Z. Tsai, W. Regan, A. Zettl, R. K. Kawakami *et al.*, Science **340**, 734 (2013).